

Review

Non-Targeted Effects of Synchrotron Radiation: Lessons from Experiments at the Australian and European Synchrotrons

Cristian Fernandez-Palomo ^{1,†}, Zacharenia Nikitaki ^{2,†} , Valentin Djonov ¹, Alexandros G. Georgakilas ^{2,*} 
and Olga A. Martin ^{1,3,4,*}

¹ Institute of Anatomy, University of Bern, Baltzerstrasse 2, 3012 Bern, Switzerland; cristian.fernandez@unibe.ch (C.F.-P.); valentin.djonov@unibe.ch (V.D.)

² School of Applied Mathematical and Physical Sciences, National Technical University of Athens (NTUA), 15780 Athens, Greece; znikitaki@mail.ntua.gr

³ Peter MacCallum Cancer Centre, Division of Radiation Oncology, 305 Grattan St, Melbourne, VIC 3000, Australia

⁴ Sir Peter MacCallum Department of Oncology, The University of Melbourne, Melbourne, VIC 3010, Australia

* Correspondence: alexg@mail.ntua.gr (A.G.G.); olga.martin@unibe.ch (O.A.M.)

† These authors contributed equally to this work.

Featured Application: The characteristics of X-rays generated at the synchrotron facilities in Australia (the Australian Synchrotron) and France (the European Synchrotron Radiation Facility) share common features which provide the basis for development of new modalities for cancer radiotherapy treatment. In addition to the empirical optimization of the physical configurations of the radiation, research is now focused on the underlying radiobiological mechanisms, especially in the context of systemic “non-targeted effects”.



Citation: Fernandez-Palomo, C.; Nikitaki, Z.; Djonov, V.; Georgakilas, A.G.; Martin, O.A. Non-Targeted Effects of Synchrotron Radiation: Lessons from Experiments at the Australian and European Synchrotrons. *Appl. Sci.* **2022**, *12*, 2079. <https://doi.org/10.3390/app12042079>

Academic Editor: Irene Paola De Padova

Received: 23 January 2022

Accepted: 15 February 2022

Published: 17 February 2022

Publisher's Note: MDPI stays neutral with regard to jurisdictional claims in published maps and institutional affiliations.



Copyright: © 2022 by the authors. Licensee MDPI, Basel, Switzerland. This article is an open access article distributed under the terms and conditions of the Creative Commons Attribution (CC BY) license (<https://creativecommons.org/licenses/by/4.0/>).

Abstract: Studies have been conducted at synchrotron facilities in Europe and Australia to explore a variety of applications of synchrotron X-rays in medicine and biology. We discuss the major technical aspects of the synchrotron irradiation setups, paying specific attention to the Australian Synchrotron (AS) and the European Synchrotron Radiation Facility (ESRF) as those best configured for a wide range of biomedical research involving animals and future cancer patients. Due to ultra-high dose rates, treatment doses can be delivered within milliseconds, abiding by FLASH radiotherapy principles. In addition, a homogeneous radiation field can be spatially fractionated into a geometric pattern called microbeam radiotherapy (MRT); a coplanar array of thin beams of microscopic dimensions. Both are clinically promising radiotherapy modalities because they trigger a cascade of biological effects that improve tumor control, while increasing normal tissue tolerance compared to conventional radiation. Synchrotrons can deliver high doses to a very small volume with low beam divergence, thus facilitating the study of non-targeted effects of these novel radiation modalities in both in-vitro and in-vivo models. Non-targeted radiation effects studied at the AS and ESRF include monitoring cell–cell communication after partial irradiation of a cell population (radiation-induced bystander effect, RIBE), the response of tissues outside the irradiated field (radiation-induced abscopal effect, RIAE), and the influence of irradiated animals on non-irradiated ones in close proximity (inter-animal RIBE). Here we provide a summary of these experiments and perspectives on their implications for non-targeted effects in biomedical fields.

Keywords: synchrotron radiation; microbeam radiotherapy (MRT); FLASH; non-targeted effects; radiation-induced bystander effect (RIBE); radiation-induced abscopal effect (RIAE); Australian Synchrotron (AS); European Synchrotron Facility (ESRF)

1. Introduction

One of the greatest advances in the field of radiation research is the evolution of the use of synchrotron X-rays in a variety of medical and biological applications, extending

to imaging, diagnostics, and radiotherapy (RT). Typical photon energies in synchrotron beams dedicated to biomedical applications range from approximately 10 to 150 keV. Currently, many synchrotron facilities operate with an electron beam energy greater than or equal to 2.4 GeV and high electron-beam currents are achievable in the accelerator ring of third- and fourth-generation synchrotrons, which include the Australian Synchrotron (AS) in Melbourne, the National Synchrotron Light Source (NSLS) in Brookhaven, USA and the European Synchrotron Radiation Facility (ESRF) in Grenoble, France, [1–3]. A table summarizing third- and fourth-generation synchrotrons around the world housing beamlines capable of conducting radiobiological and clinical research is presented in Supplementary data (Section S1). Operation principles of synchrotrons are presented in Supplementary data (Section S2).

The ESRF shares a physical site, called the European Photon and Neutron Science Campus, with the neutron source Institut Laue-Langevin and the European Molecular Biology Laboratory. The AS is a major research facility located in Clayton, a technology and innovation hub of southeast Melbourne. The AS belongs to the Australian Nuclear Science and Technology Organization (ANSTO), which is a statutory body of the Australian government, formed in 1987 to replace the Australian Atomic Energy Commission. Currently, AS and ESRF facilities are best configured for a wide range of biomedical research studies, including animals and potentially human cancer patients in the future.

In this review, we discuss the properties of synchrotron X-ray beams that are essential for generation of novel radiation modalities and their applications for radiobiology and medicine. Synchrotron-based RT is, so far, preclinical, but has great potential to improve outcomes of cancer RT [4–6]. Studies on non-targeted effects of X-ray synchrotron RT are scarce. In recent years, our groups have conducted such studies at the Imaging and Medical Beamline (IMBL) of the AS and at the Biomedical Beamline (ID17) of the ESRF. Here, we summarize our findings and outline perspectives for future studies and implications in the biomedical arena.

2. Characteristics of Synchrotron X-rays at AS and ESRF

The key characteristics of synchrotron X-rays relevant for radiobiology include:

- The high brightness, or brilliance, which describes synchrotron radiation power. Brilliance measures the source quality and implicates the number of photons produced per second. The higher the brilliance value, the stronger the emitted beam.
- The low divergence of the synchrotron beam enables the irradiation of the target with collimated parallel microbeams, in contrast to conventional RT. The low divergence results from the fact that the target is several meters away from the permanent magnet wiggler which generates the X-ray beam. At the AS, the distance between the wiggler and the target is about 32 m, while at the ESRF it is 40 m.
- The beam current, which is the basic quantity of the beam. In this regard, the ESRF's characteristics are superior to those of the AS. The ESRF has a significantly longer periphery of 844 m, while the AS has 200 m. The brilliance values are 8×10^{20} and 4.6×10^{18} photons/(s \times 0.1% bandwidth \times mrad²) for the ESRF and AS, respectively [7]. Both have a beam current of 200 mA; however, the maximum electron energy is 6 GeV for ESRF and 3 GeV for AS.
- The intense flux (dose rate) of photons allows samples to be irradiated very quickly in the range of seconds and milliseconds. Dose rates in the AS range from 30–1000 Gy/s, while at the ESRF can be up to 16,000 Gy/s.
- The energy of the synchrotron beam is in the KeV range, which has the advantage of allowing for low secondary electron (Compton) scattering. The energy range at both the AS and ESRF is “tunable”, meaning, the energy spectrum can be filtered to remove low energy photons and use a poly energetic X-ray beam typically between 30 and 120 KeV.

These physical properties enable the development of new spatially fractionated RT (SFRT) such as microbeam RT (MRT) and FLASH RT, which are described below.

3. Synchrotron-Generated Novel RT Modalities

3.1. Microbeam Radiation Therapy (MRT)

Biomedical beamlines at synchrotrons can generate both uniform (broad beam, BB) radiation fields as well as spatially fractionated fields (Figure 1). The radiation field can be spatially fractionated by adding a multislit collimator to the beam path. This generates an array of planar X-ray microbeams, typically only tens of μm thick, separated by gaps of a few hundred μm [8]. This array of microbeams is known as MRT and is used to target tumors in animal models. MRT shows significant promise for increased tumor control and reduced normal tissue damage compared to conventional RT. Synchrotrons can generate such high dose rate X-ray microbeams with physical properties superior to conventional sources [9].

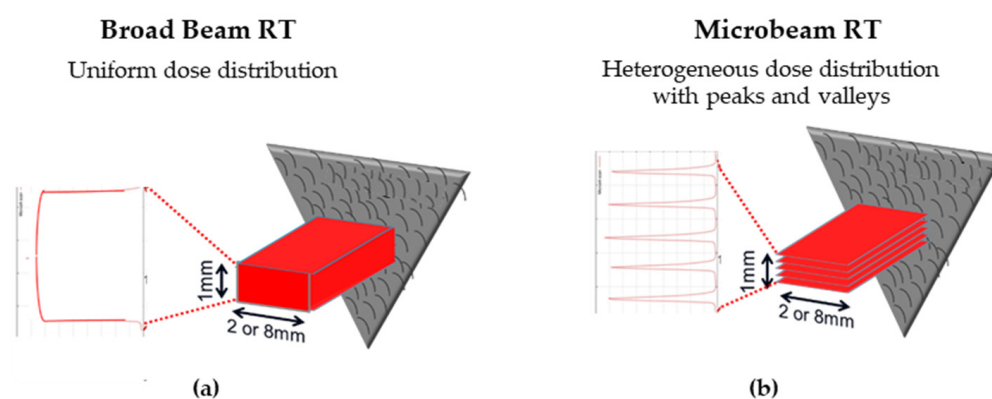


Figure 1. Synchrotron can generate both broad beams and microbeams. (a) Broad beam synchrotron RT is a type of conventional RT which uses spatially uniform dose distribution. (b) MRT has a heterogeneous dose distribution with ablative peak and low valley doses. Typical beam dimensions used in the AS experiments are described below.

The MRT collimator normally produces planar microbeams of 25 or 50 μm thick spaced by 200 or 400 μm center-to-center in the horizontal dimension. In the vertical dimension, the microbeam array is just a few mm high (between 0.3 to 1.5 mm). However, this can be extended by using the goniometer stage to scan the sample vertically through the beam, and thus extending the microbeam array several cm. The multislit collimator then generates a heterogeneous dose distribution, where hundreds of Gy are delivered directly by the microbeams (“peak doses”) with regions between them receiving low-dose scatter irradiation (“valley dose”). However, this heterogeneous dose distribution depends on factors such as the energy spectra inherent to the synchrotron facility:

- The main clinical research focus at the IMBL, AS, are RT and imaging. Imaging can be performed in an energy range of 15–150 KeV, while radiotherapy can be performed in an energy range of 30–120 KeV and with dose rates close to 1000 Gy/s [10]. The radiation source of MRT is a wiggler with a peak magnetic field of 4.2 T [11]. Starting from a storage ring current of 200 mA, a standard MRT spectral configuration can be delivered in 300 Gy/s by setting the wiggler to 3 T, which produces a spectrum with an average energy of 94 KeV and a peak energy of 87 KeV. Another MRT configuration can deliver 991.7 Gy/s by setting the wiggler to 4 T, with similar spectra as above (93 KeV on average) [12].
- The ESRF’s beamline ID17 is also intended for medical imaging and RT studies. The radiation used for MRT comes from a wiggler of 1.5 m in length and a magnetic field of 1.6 T at a gap of 24.8 mm. The X-ray beam produced by the wiggler then continues for 37 m until it is attenuated to produce one of three different spectral configurations:

(i) the standard MRT configuration used for rodent experiments for many years has an average energy of 104.2 KeV and a peak energy of 87.7 keV, (ii) the preclinical MRT configuration developed for veterinary trials and has a mean energy of 119 KeV and a peak energy of 102.1 KeV, and/or (iii) the clinical MRT configuration for future clinical applications with a mean energy of 122.8 KeV and a peak energy of 108.2 KeV [3,13].

Synchrotron radiation is required for MRT because: (i) the minimal beam divergence maintains the microbeam geometry at the microscopic level, (ii) the X-ray energy spectrum of 80–150 keV minimizes the range of secondary electrons that make an important contribution to the valley dose, and (iii) the ultra-high dose rates avoid beam smearing due to the cardiovascular movement [14]. The use of ultra-high dose rates has another advantage, namely the reduced radiation toxicity of normal tissue due to the rapid irradiation. This phenomenon is called the FLASH effect and is considered one of the most promising recent advances in radiation oncology.

3.2. Ultra-High Dose Rate Radiotherapy (FLASH-RT)

FLASH-RT delivers large single doses of radiation (10–30 Gy) with ultra-high dose rates, in less than 500 ms [15]. The whole idea lies on preliminary theoretical and experimental results showing very low normal tissue toxicity enabling dose escalation and thus enhanced tumor control. Within this context, FLASH-RT is considered for electrons and protons, but also photons [16]. The normal tissue sparing effect, the “FLASH effect”, prevents lung and brain toxicity, based on studies in several cellular or animal models [17]. Recently, it was confirmed that FLASH-RT spared normal rat brain from radiation-induced cognitive impairment when the overall irradiation time was less than 200 ms [15]. The FLASH effect has been shown to occur in pig’s skin and squamous cell carcinoma (SCC)-bearing cat patients irradiated within a phase I veterinary clinical trial [18,19], indicating the treatment potential for human patients. High radiotolerance of normal tissues was observed using X-ray micro or broad beams delivered in a FLASH mode [20]. Recent results from the AS underline the pivotal role of the very high dose rate [21]; the toxicity of synchrotron and conventional RT was compared, based on a total and partial body irradiation in mice. The results indicate no normal tissue sparing effect at 37–41 Gy/s in contrast to studies with a very high dose rate of ≥ 100 Gy/s [21]. The 10 Gy broad beam whole-brain irradiation of mice or rats with synchrotron generated X-rays (mean dose rate of ~ 17 kGy/s) did not induce memory deficits up to 6 months after exposure compared to standard dose rates of ~ 0.05 Gy/s [16].

3.3. MRT Delivered in a FLASH Mode

Micrometer collimation allows for the application of hecto-Gy doses and is the basis for the FLASH-mode MRT [22] (Figure 2). A highly heterogeneous pattern of high and low radiation doses is delivered simultaneously in just a few milliseconds thanks to the ultra-high dose rates of the synchrotron facilities (up to 16 kGy/s). Compared to conventional RT, this MRT dose delivery pattern has been proven to (i) spare various normal tissues from radiation-related toxicity [6], and (ii) efficiently eradicate local tumors [23] (Figures 3 and 4).

Studies of synchrotron MRT in animal models indicated that tumors can be ablated by MRT at radiation levels that spare normal tissues [8,24–26]. Thus, the therapeutic index for MRT is greater than conventional RT, and it is quite conceivable that MRT may become a major mode of cancer RT in the future. Recently, the first dog patient treatment of spontaneous glioma was successfully treated at the ESRF (report pending), and issues surrounding the clinical implementation of MRT have been discussed in several publications [20,22,27,28]. The reason for the beneficial difference in response to MRT in tumors and normal tissues are being actively investigated, with inter-cellular effects between maximally and minimally irradiated cells in the peak and valley regions implicated [9,24,29]. An integrated knowledge of the effect of MRT on tumor and normal tissues can be summarized as follows:

- MRT has been proven to be an efficient treatment strategy for several tumor types in animal models, including glioma, glioblastoma, mammary carcinoma, melanoma, squamous cell carcinoma and lung cancer [23].
- A fractionated MRT schedule controls the primary tumor better than a single MRT treatment [26,30,31].
- MRT has been proven to efficiently spare normal tissues of the central nervous system (CNS, including immature CNS), skin, liver, lung, liver, vasculature and testis from detrimental effects of radiation [6,12].
- The higher the dose rate, the better the normal tissue sparing effect [16,32].
- MRT valley doses correlate best with lower acute normal tissue toxicity [21,23].
- MRT selectively destroys tumor neovasculature leading to tumor hypoxia and necrosis, while vasculature in normal tissues is more tolerant and, if damaged, can repair itself. This contributes to differences in survival between tumor and normal tissues [33–35].
- Ultra-high doses of MRT beams are likely to induce high DNA damage-generated ‘immunogenic cell death’, as has been suggested for FLASH irradiation [36].
- Similar to the activation of the immune system after heterogenous dose delivery with conventional-source SFRT [37], immune cells in the valleys are spared following MRT and can activate an anti-tumor immune response (manuscript under review). In addition, short-pulse FLASH mode is capable of protecting the majority of local and circulating immune cells [36], thus further contributing to the active recruitment of immune cells to the microbeam paths.
- MRT promotes an anti-tumor immune response that contributes to exceptional killing of the primary tumor [38]. We recently showed that fractionated MRT-induced immunomodulation is associated with a pronounced decrease in metastasis (manuscript under review). The ability of local MRT to trigger immune-mediated, systemic, non-targeted radiation effects can contribute significantly to the future clinical utility of this irradiation modality.

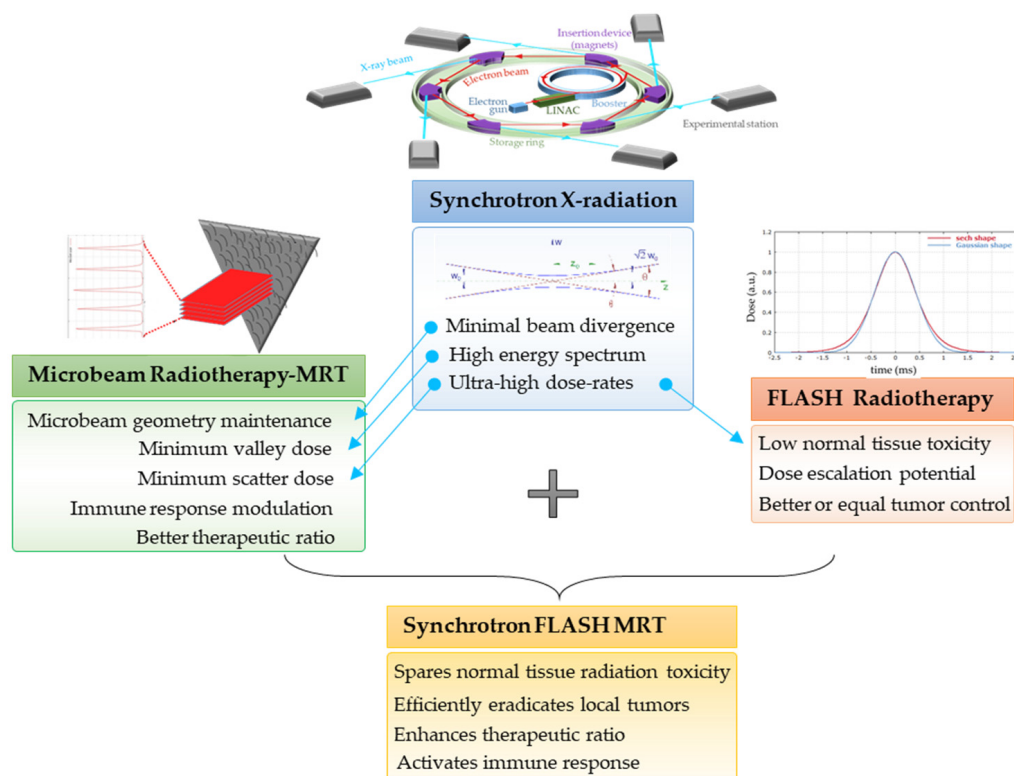


Figure 2. Synchrotron X-ray radiation properties are essential for both MRT and FLASH RT. Synchrotron MRT in FLASH mode is the combinatorial result of MRT and FLASH RT, whose properties dictate its therapeutic potential.

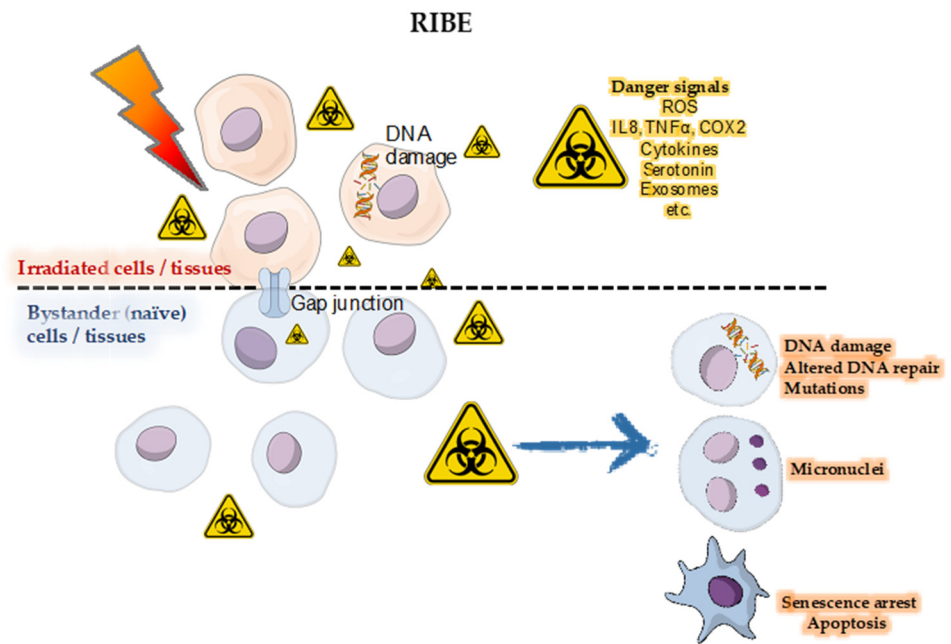


Figure 3. Radiation-induced bystander effect (RIBE). Directly irradiated cells produce danger signals inducing DNA damage and cell death in adjacent, non-irradiated cells. The latter are called bystander or naïve cells.

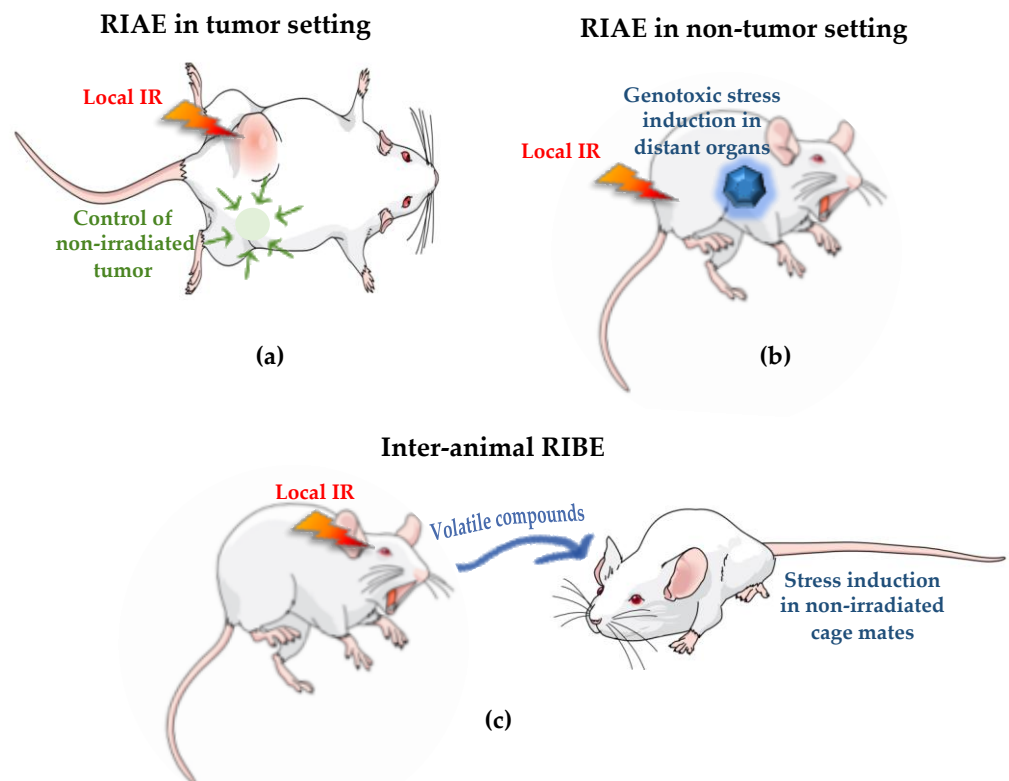


Figure 4. Non-targeted effects in animals that can be generated at synchrotron facilities. RIAE within the same organism in tumor (a) and non-tumor settings (b) display different systemic effects mediated by the immune system. RIAE can be both beneficial (a) or genotoxic (b). (c) Detrimental or beneficial non-targeted effects mediated by volatile factors can occur in another bystander organism(s) sharing an environment with irradiated animals (see Section 5.2.2).

4. Radiation-Induced Bystander and Abscopal Effects

4.1. Studies of RIBE and RIAE and Their Mediators

Cancer RT is based on the dogma that radiation kills targeted cells. This dogma is challenged by the radiation-induced bystander effect (RIBE), in which unirradiated (naïve) neighboring cells can also be damaged after receiving signals from irradiated populations, whether through direct cell-to-cell contact or exposure to conditioned medium (Figure 3) [39–42]. RIBE is now a well-established consequence of ionizing radiation and manifests as increased genomic abnormalities and loss of viability of ‘naïve’ cells. Nagasawa and Little [43] published the first modern report on RIBE. Their data showed that alpha particles directed at 1% of a given cell group induced sister chromatid exchanges in 30% of that population. The authors supported their findings with statistical data showing that the proportion of cells damaged by a single alpha particle was less than the number of cells that exhibited sister chromatid exchanges. Later it was discovered that the targeted cells release damage-inducing substances into the medium, and medium conditioned by irradiated cultures was shown to induce various types of genotoxic events in unirradiated cultures [40].

Researchers in this field agree that the induction of RIBE is mediated by signals transmitted from irradiated cells to non-irradiated cells [44,45]. Bystander effects are known to be communicated in two ways, both discovered around the same time by different researchers. The first is by gap-junction intercellular communication [42], and the second is extracellular soluble factors [41]. These mechanisms were the only known communication pathways for several years until it was recently discovered that UV photons from irradiated cells can also trigger bystander responses [46,47].

Affected bystander cells exhibit increased levels of micronuclei, apoptosis, mutations, altered DNA damage and repair, senescence arrest [40,48], and increased levels of phosphorylated histone H2AX (γ -H2AX) [49], a marker of DNA double-strand breaks (DSBs) [50–52]. In contrast to DSB dynamics in irradiated cells, where maximal γ -H2AX signal is observed 30 min after irradiation, foci formation is delayed in bystander cells. In 3D tissue models irradiated with microbeams, the maximal number of γ -H2AX foci was observed 12–48 h after irradiation and gradually decreased over 7 days [51].

Mediators of RIBE include several inflammatory cytokines that were found at elevated levels in the medium conditioned by irradiated cells [53,54]. The cytokine TGF- β , when added to cell cultures, induced increased DSB levels similar to those induced by the conditioned medium [55]. IL-8 was found to be associated with an increase in ROS [56], which itself plays a role in RIBE [57–59]. In addition to ROS and NAD (P)H oxidase, TNF- α was also found to be involved in the bystander signaling process [60]. Nitric oxide was found to play a role in the bystander signaling process when cell proliferation was induced in neoplastic human salivary gland cells [61,62]. Increased radioresistance was observed in p53 wild-type glioblastoma cells [63] after exposure to nitric oxide-containing conditioned media. COX2 [64] and serotonin [65] have been implicated in the process of bystander signaling, with the latter confirmed by several publications [66–69]. Recent research has shown that long-noncoding RNAs contained in exosomes are bystander candidates [70–72], while UV photons are the only physical factor shown to induce bystander effects [46,47].

Although RIBE are usually considered detrimental to the cell, there are also reports of protective bystander effects in vitro, such as (i) bystander signaling leading to a reduction in neoplastic transformation [73] and (ii) evidence that bystander effects trigger adaptive responses [74,75]. In fact, for decades, radiation oncologists have reported reactions in normal, unirradiated tissues after RT. These “out-of-field”, or abscopal effects have been described as “an action at a distance from the irradiated volume but within the same organism” [76]. The discovery of the RIBE has prompted the description of radiation-induced abscopal effects (RIAE) as distant in vivo bystander effects, and their further investigation. Several studies reported in vivo RIAE in animal models. Using strategies that involve partial head or body 1 Gy X-ray irradiation, profound genetic and epigenetic changes were identified in shielded organs, such as skin and spleen [77,78]. Others reported

DSBs, apoptosis, and tumor induction in shielded cerebellum of 3 Gy X-ray-irradiated radiosensitive Ptch1 heterozygous mice [79]. Strikingly, the results of the *in vivo* non-targeted effects can be transmitted to future generations. While genomic instability was known to be elevated in offspring of parents whose germ cells were directly irradiated prior to conception as part of a medical procedure [80], male rats given cranial irradiation (20 Gy applied as two doses of 10 Gy on two consequent days) had an accumulation of unrepaired DNA damage in their sperm cells [81]. This effect was manifested as epigenetic dysregulation in the unexposed progeny conceived after paternal exposure. RIBE and RIAE are potential contributors to the well-documented clinical phenomenon of secondary cancers, a major concern in cancer RT, affecting more than 1% of patients [40,82].

Clinically, patients often suffer from systemic side-effects, such as fatigue, diarrhea, and weight loss during local RT. Additionally, RIAE can cause damage to a distant, non-irradiated tumor [83]. The reported instances of spontaneous anti-tumor abscopal effects following local RT as a sole therapy are rare. In a review by Siva et al. [84], 10 cases of abscopal effects in RT patients with a range of solid tumor types were reported, and in another review, 35 cases over 45 years were reported, out of millions of patients treated during this period [85]. The clinical reports of anti-tumor RIAE have covered a wide range of doses given in either single or multiple fractions; however, they are more prominent following larger doses, supporting the use of hypofractionation [86].

Most published studies of RIAE in animals and patients describe biological effects observed in distant, non-irradiated normal or tumor tissues (Figure 4a,b). However, published data also describes the transmission of bystander signals from one irradiated animal to another non-irradiated animal (Figure 4c). The first observation of such inter-animal communication was made when non-irradiated rats and mice were placed in the same cage with irradiated animals for one to two weeks [87]. The researchers observed that the peripheral blood of the non-irradiated animals showed a marked decrease in leukocytes and a lower immune reactivity. A similar communication was also shown between fish [88]. In these experiments, unirradiated rainbow trout showed bystander effects after swimming with trout that had been exposed to radiation. This was later confirmed in zebrafish [89] and with proteomic analysis of non-irradiated, bystander rainbow trout [90]. Bystander responses have also been found to persist throughout the lifespan of fish after they have been irradiated in the early life stages [91]. Below, we review the studies conducted at the AS and ESRF facilities to explore various types of non-targeted effects of ionizing radiation and summarize the biological mechanisms discovered.

4.2. First RIBE Studies at Synchrotrons

Bystander effects are important in synchrotron radiation because tissues exposed to valley doses also receive the signals emitted by cells in the peak dose regions and vice versa. Research on the relevance of these bystander effects in synchrotron RT has a traceable history of no more than 14 years. The first study to suggest that bystander effects play an important role in synchrotron MRT was published by Dilmanian et al. [24]. In their experiments, the team irradiated bovine aortic endothelial cells and rat spinal cord with MRT. The results showed that the elimination of apoptotic cells and repair processes were faster than expected. This finding suggests that “beneficial” bystander factors are involved in tissue repair by promoting proliferation, migration, and differentiation of progenitor cells in the spinal cord. However, there are previous studies showing an increase in cell proliferation [92] and radiation-induced changes in the immune response of local immune cells and tumors [93], but these have not been associated with bystander effects.

Kashino et al. [94] provided further evidence for bystander effects by examining the response of the C6 glioma cell line to synchrotron micro-beams. The authors observed a higher number of DNA DSBs in cells adjacent to the irradiated area than would be expected from scattered radiation alone. They also noted cellular migration into the zones irradiated with peak doses. The team confirmed the role of RIBE by exposing unirradiated cells to the conditioned medium and observed a marked increase in 53BP1 foci.

Tomita et al. [95] found that normal human fibroblast WI-38 cells that had been exposed to synchrotron microbeams induced cell death in unirradiated cells. The authors confirmed their finding by treating WI-38 cells with aminoguanidine (an inhibitor of nitric oxide) before irradiation, which abolished the bystander effects and thus cell death. Another study published by the same group [96] showed that synchrotron-induced bystander effects were also observed in Chinese hamster V79 lung cells and that they could also be abolished by using nitric oxide inhibitors.

The studies by Tomita, Maeda, and team [95,96] also showed clonogenic bystander survival characterized by high cell killing at low doses followed by a marked escalation of survival with increasing doses. The authors described this response as a parabolic increase in bystander cell death. This is a well-known response in radiation biology and is known as low-dose hyper radiosensitivity (HRS) and increased radioresistance (IRR).

5. RIBE and RIAE Studies at the AS and ESRF Synchrotron Facilities

5.1. Studies at the AS

5.1.1. In Vitro RIBE Studies at the AS

Earlier reports of bystander endpoints following partial irradiation of animals with conventional X- or γ -rays have attracted criticism asserting that the observed effects may have been due to low doses of scattered radiation, rather than true bystander signaling. To address this possibility, RIBE experiments were conducted at the IMBL at the AS by Martin's team [97,98]. The design of irradiations was such that a defined zone of a cell population grown in one well of a two-well chamber slide was irradiated with various doses of MRT or BB at the dose rate of 49.3 Gy/s. The chambers were divided by a plastic wall; therefore, the cells grown in the non-irradiated well were separated from the irradiated cells and not exposed to the factors that the irradiated cells secrete to the medium. Scoring of γ -H2AX foci in different cell populations—directly irradiated, out-of-the irradiated zone bystander cells in the irradiated well, and separated cells in the non-irradiated well—allowed a quantitative analysis of the impact of scattered radiation on the cellular response.

Doses of scattered radiation were determined by a sensitive radiochromic film XRQA2 dosimetry at various distances from the irradiated zone. As expected, the scattered dose at the given distance correlated with the absorbed dose in the irradiated zone measured by a radiochromic film, EB3. The sensitivity of the γ -H2AX assay was sufficient to measure as low as 0.01 Gy of scattered radiation at 30 min post-exposure [97], the time point that corresponds to maximum foci formation. Therefore, while the γ -H2AX assay has not been shown to be an appropriate biodosimeter for MRT valley doses [99], it seems to be good for estimating the effects of scattered radiation after exposure of biological targets to synchrotron radiation. This quantification provided a tool for answering an important question: whether scattered radiation contributes to the appearance of RIBE.

Lobachevsky et al. [97] observed RIBE (manifested as increased DNA damage measured by γ -H2AX foci) in naïve human keratinocytes sharing medium with the cells in the irradiated well. An overall trend for a larger number of γ -H2AX foci was observed in bystander cells compared to the cells in a separated well, only affected by scattered radiation. In the following study by Lobachevsky et al. [98], human colon cancer cells were subjected to the similar study design as described above for MRT and BB irradiations. Scattered radiation substantially contributed to overall DNA damage accumulation in naïve cells sharing medium with irradiated cells. Moreover, the cells exposed to the low-dose scatter also generated unreparable DNA damage, possibly due to an ongoing exchange of bystander signaling induced by low dose-irradiation. A more pronounced bystander response was observed in unirradiated cells co-cultured with cells exposed to BB compared to MRT. A question as to whether loss of p53, the major tumor suppressor gene [100], would modify DNA damage response in non-irradiated cell cultures was also addressed. For p53-null cells, an overall reduced response to low-dose scatter irradiation, but not for RIBE, was detected. As a clinical implication, slower DNA damage repair and maintenance of unreparable DNA damage in out-of-field tumor and normal tissues

may cause over-sensitivity to low-dose scattered radiation in cancer radiotherapy patients, especially those carrying p53 deficiencies. Since p53 plays a central role in DNA damage responses, such as cell cycle arrest, senescence, apoptosis, and DNA repair [101,102], the implication may be valid for deficiencies in the related genes.

5.1.2. In Vivo RIAE Studies at the AS

In the absence of a tumor, we compared the induction of RIAE following local MRT irradiation and BB field synchrotron X-ray irradiation in mice to establish whether MRT also induces long-range RIAE. A thorough study of RIAE as a function of irradiated tissue volume, radiation dose, beam configuration and time has never been performed before. We extended the investigation of the RIAE by determining the influence of these parameters on its propagation by tracking the kinetics of its appearance. The overall experimental strategy was to choose the irradiation parameters which produce the most robust RIAE by investigating the effect of irradiated tissue volume, dose, and time. Based on the results, optimal irradiation parameters were then used to establish the extent of RIAE in immune-compromised mice, in order to understand the role of the immune system in RIAE propagation.

Young C57BL/6J female mice were positioned in a specially designed jig so that only the right flank was exposed during irradiation. Skin on the right hind leg was irradiated with a short pulse of MRT or BB (200 and 810 ms for 10 and 40 Gy peak dose with dose rate of 49 Gy/s) [103]. Energy deposition was assessed by analysis of incident and exit doses using radiochromic film affixed to the skin. Scattered radiation was measured in the organs of interest and its ability to directly induce cellular responses was found to be negligible. Both radiation modalities were equally capable of inducing significant and persistent effects to normal, out-of-field tissues in mice, attributed to RIAE. These effects included elevated γ -H2AX foci indicating DNA DSBs, apoptosis, local oxidative stress, inflammation and senescence, and decreased proliferation in the out-of-field duodenum, a highly proliferative tissue that is vulnerable to the systemic cell–cell signaling induced by a local stressor [55,104]. Oxidative clustered DNA lesions (OCDL) were elevated in various tissues throughout the body. Local and systemic immune responses were also induced. The innate immune response, i.e., increases in macrophages/dendritic cells (DC) and neutrophils, was observed in the irradiated skin, while in out-of-field duodenum both the innate and adaptive immune response (macrophages/DC, neutrophils, and T-cells) were activated. Significant alterations in a range of plasma cytokines including CSF1R, IL-10, TIMP1, VEGF, TGF β 1, and TGF β 2 were also observed, which likely affected activation of other factors responsible for the propagation of RIAE.

Under a similar irradiation procedure, skin of mice with a range of immune system abnormalities was irradiated with 10-Gy peak dose MRT to identify which components of the immune system were essential RIAE mediators [105]. These immune-deficient mice were: SCID/IL2 γ R^{-/-} (NOD SCID gamma or NSG) mice that lack mature T and B lymphocytes and natural killer (NK) cells; C57BL6/J wild-type (WT) mice treated with an antibody that neutralizes CSF-1R, which is expressed on monocytes and monocyte-derived macrophages/DC at sites of inflammation produced by tissue injury; and C57BL6/J mice deficient in CCL2/MCP1, a member of the C-C chemokine cytokine family that recruits monocytes, memory T cells, and macrophages/DC to sites of tissue injury. C57BL6/J WT mice served as a control cohort. CCL2 KO mice were of particular interest as CCL2 plays a role in inflammation-related diseases [106] and has been implicated in the progression and prognosis of several cancers [107]. The blockade of CCL2 can inhibit tumor growth of primary and metastatic disease in animal cancer models [108]. CCL2 is also involved in elevated COX-2 production and TGF- β up-regulation [109], both critical factors in bystander signaling and carcinogenesis [40]. In non-irradiation settings, when tumors were implanted into C57BL6/J WT and CCL2 KO mice, there was no measurable increase in distant DNA damage in the tumor-bearing CCL2 KO mice, while DSB and OCDL were

elevated in distant tissues of WT mice [104]. Thus, CCL2 was essential in the tumor-induced systemic genotoxic response *in vivo*.

Little or no change in DNA damage and apoptosis was observed in out-of-field tissues of the immune-deficient mice after local MRT exposure, proving that RIAE relies on the functional immune response [105]. No change in DNA damage and apoptosis was observed between CCL2 KO mice and WT mice injected with anti-CSF1R neutralizing antibody, which renders mice macrophage-depleted, indicating that macrophages and CCL2 play key roles in generation and propagation of RIAE. We speculate that CCL2, induced at the irradiated site, attracts macrophages that secrete more CCL2 and TGF β , that bind to their receptors, CCR2 and TGF β R1, in out-of-field tissues. CCL2 then creates a site of local inflammation by activating tissue-associated macrophages (TAM). ROS at the abscopal site can be generated directly by TAM, or via TGF β production. CCR2 also up-regulates TGF β . Subsequently, TGF β promotes RIAE, including DNA damage and apoptosis. Therefore, targeting the innate immunity via CSF1R in macrophages and/or blocking TGF β and CCL2 could potentially protect out-of-field tissues from non-targeted systemic effects of IR [105,110].

Finally, out-of-field (i.e., 35 mm from the irradiated site) skin samples were collected in both aforementioned studies for gene expression analysis [111]. The influence of irradiated target size, dose, and beam modality (MRT and BB) on gene expression was investigated in both C57BL6/J WT and CCL KO mice. Gene expression changed in six genes, Tgf β , Tp53, Tnf, Ccl2, Ccl22, and Mdm2, with a degree of independence from dose and radiation modality. Particularly significant were an increase in Tnf expression and a decrease in Mdm2 expression, genes associated with inflammation, including macrophage activation [112], and DNA damage. In CCL2 KO mice, gene expression profile exhibited an early increase in Mdm2, Tgf β 1, Tnf and Ccl22 expression that was not observed in the immune-proficient mice. Therefore, the innate immune system is involved in out-of-field tissue responses and alterations in the immune status change the tissue response to RIAE.

5.2. Studies at the ESRF

5.2.1. In-Vivo RIBE/RIAE Studies at the ESRF

The first set of experiments at the ESRF demonstrating that RIBE play a role in the heterogeneous dose distribution of MRT began with work on rats performed by the Mothersill lab [113]. In this study, brain tissue and urinary bladders were harvested from irradiated and nonirradiated Wistar rats and cultured as tissue explants to produce conditioned media containing potential bystander signals. This explant-conditioned media were then added to HPV-G cells, which “reported” the occurrence of bystander effects by decreasing their colony-forming capacity. For this experiment, the right hemisphere of the brain of normal and tumor-bearing rats was irradiated with MRT at peak doses of 17.5, 35, 70, or 350 Gy. This dose-escalation approach is important because, until then, bystander effects had been associated only with low doses of radiation. The results showed that all MRT doses directed to the right hemisphere resulted in bystander effects, regardless of whether the animals were tumor-free or tumor-bearing. In addition, unirradiated abscopal tissue (left hemisphere and urinary bladder) also resulted in RIBE in the reporter cell line. This was an important finding, because it showed that RIBE, normally thought to occur in the vicinity of cells, could also be a systemic effect. The team then published another study examining proteomic changes in the rat brain triggered by MRT-induced RIBE [114]. The results showed that bystander effects after MRT dose peaks of 35 or 350 Gy appear to have a protective effect on the animals. Specifically, the team uncovered an anti-tumor bystander proteomic signature directly related with ROS-induced apoptosis. This bystander signature confirmed previous studies from rainbow trout overexpressing protective proteins after exposure to bystander signals [90].

In a similar study design, Fernandez-Palomo et al. paid special attention to the induction of non-targeted effects in animals with a weakened immune system [115]. In these experiments, the brains of athymic mice were implanted with F98 glioma cells and irradiated at the ESRF with MRT and a series of collimated pencil beams (PB). Peak doses of 200 Gy for MRT and 1000 Gy for PB were used to irradiate the entire brain. The results showed that the presence of the F98 tumor in the immunocompromised mice abrogated both RIBE and RIAE. This strongly suggests that a healthy immune system or part of its cellular pathway is necessary for RIBE and RIAE to take place, in agreement with the results of aforementioned studies conducted at the AS [105].

Another set of experiments on rats bearing glioblastomas explored the use of the γ -H2AX as a marker for dose deposition after synchrotron MRT, which also revealed a role of bystander effects in spatially fractionated radiation [116]. MRT was administered to the right hemisphere of rats in the form of an array of 50 microbeams with a width of 25 μ m and a distance of 200 μ m center-to-center, while delivering peak doses of 35, 50, or 350 Gy. Quantification of the occurrence of DNA damage by way of γ -H2AX, showed a 1.8-fold increase in the width of the microbeam track compared with its original size (from 25 μ m to 45 μ m) 4 h after peak MRT doses of 350 Gy. At 8 h after MRT, the width of the microbeam track further increased to 2 times its original size (from 25 μ m to 50 μ m). This increase in γ -H2AX immunoreactivity over time is clearly independent of direct radiation injury and can currently only be explained as a bystander effect originating from cells exposed to both the high peak doses and the dose gradient in the transition zone. This RIBE would then amplify DNA damage and manifest itself as broader γ -H2AX tracks.

5.2.2. Inter-Animal Communication of RIBE at the ESRF

The Mothersill laboratory examined a concept first proposed by Surinov [117], who hypothesized that irradiated animals have the ability to communicate stressors via volatile compounds (Figure 4c). Surinov's original study showed, first, that the urine of irradiated mice and rats was the source of the bystander signals and, second, that no physical contact between the urine and naive mice and rats was required for transmission of the bystander signals. They confirmed the latter by removing the bedding of the irradiated animals and placing it under the cage of the non-irradiated mice and rats. The bystander animals exhibited lower immunoreactivity than the control animals. Thus, since there was no physical contact, the bystander signals, which are yet to be identified, must have been transmitted via volatiles.

There are no publications about specific chemical signals of pathological states and their effects on intact animals. The only exception are reports about "fear smell" release by stressed animals; this smell modifies the immunity of intact animals [117,118]. Surinov et al. [117] speculate that under physiological conditions, syngeneic secretions can be attractive, while allogeneic secretions are immunosuppressive to intact animals. Presumably, this is a manifestation of emission of different chemical signals, with a biological purpose associated with the natural selection. At least in plants, methyl salicylate (MeSA) and methyl jasmonate (MeJA) serve as volatile signals communicating genome instability (as measured by an increase in the homologous recombination frequency) between UVC-irradiated plants and their unexposed neighbors [119].

In the study conducted by Mothersill's team at the ESRF, Wistar rats exposed to localized BB or MRT were placed in the same cage with unirradiated animals [120]. After 48 h, the BB and MRT-exposed rats, as well as the unirradiated "cage-mates" were euthanized and tissues were collected to produce explant-conditioned media for the clonogenic reporter assay. Their results confirmed the transfer of bystander factors from the irradiated rats to completely unirradiated rats. This work was complemented by a subsequent study in which the bystander proteome was examined. BB radiation increased serum albumin, heat shock protein 71 (HSP-71), triosephosphate isomerase (TPI), fructose bisphosphate aldolase (FBA), and prohibitin and decreased dihydrolipoyl dehydrogenase (DLD) and pyruvate kinase in exposed animals. MRT-exposed animals demonstrated increased HSP-71, FBA,

and prohibitin, and decreased aconitase, dihydropyrimidinase, TPI, tubulin DLD, and pyruvate kinase. The cage mates with BB irradiated rats showed increased HSP-71 and FBA and decreased pyruvate kinase, DLD, and aconitase, indicative of tumorigenesis. The cage mates of MRT-irradiated rats showed an increase in HSP-71, prohibitin, and FBA, and decreased aconitase and DLD, which, the authors believe, is indicative of an oxidative stress response and an antitumor bystander proteome that could also confer radioresistant properties.

6. Conclusions

In conclusion, extensive data have accumulated over the years on studies of RIBE and RIAE generated by synchrotron sources. While the results are largely consistent with those obtained after irradiation by conventional sources, there are several areas that should be investigated further. First, it is important to decouple the role of peak doses, valley doses, and transition zone doses in the induction of signaling molecules. Perhaps next-generation sequencing focusing on spatial transcriptomic analysis could shed more light on these mechanisms. Second, synchrotron facilities are capable of delivering MRT at ultra-high dose rates, but the studies reviewed here largely do not consider FLASH-RT; only generated non-targeted effects. This is a limitation of our review, but we believe that this vacuum is rooted in the fact that the FLASH effects have only recently been rediscovered. Therefore, it would be of great importance to re-evaluate some results with special reference to dose rate. This reevaluation could shed more light on interesting findings such as the protective bystander proteome or the involvement of the immune system in RIAE.

Supplementary Materials: The following supporting information can be downloaded at: <https://www.mdpi.com/article/10.3390/app12042079/s1>, Section S1: Third and fourth generation synchrotrons that conduct radiobiological and clinical research. Section S2: Synchrotrons' operation principles. References [121–125] are cited in the supplementary materials.

Author Contributions: Conceptualization, A.G.G. and O.A.M.; investigation, C.F.-P. and Z.N.; writing—original draft preparation, O.A.M., C.F.-P., Z.N.; writing—review and editing, all authors; funding, O.A.M. and V.D. All authors have read and agreed to the published version of the manuscript.

Funding: The support was provided by the Australian National Health and Medical Research Council (NHMRC) grant 10275598 and Swiss Cancer Research foundation grant KFS-4281-08-2017. Z.N. contribution was co-financed by Greece and the European Union (European Social Fund-ESF) through the Operational Programme “Human Resources Development, Education and Lifelong Learning”, under the “2nd Call for Research Projects for Postdoctoral Researchers” (MIS 5033021), implemented by the State Scholarships Foundation (IKY).

Institutional Review Board Statement: Not applicable.

Informed Consent Statement: Not applicable.

Data Availability Statement: The authors confirm that the data supporting the findings and suggestions of this study are available within the article and available from the corresponding authors upon logical requests.

Acknowledgments: All authors would like to express their sincere thanks to Jennifer M. Fazzari (University of Bern) for careful reading of the manuscript and helpful suggestions. We also thank ANSTO and the AS for use of the IMBL beamline and facilities and the ESRF for use of the ID17 beamline and facilities, where the described experiments have been conducted.

Conflicts of Interest: The authors declare no conflict of interest.

Abbreviations

ANSTO	Australian nuclear science and technology organization
AS	Australian synchrotron
BB	Broad beam
CCL2/MCP1	Chemokine ligand 2/monocyte chemoattractant protein-1
CCL22	Chemokine ligand 22
CCR2	Chemokine ligand 2 receptor
CERN	European organization for nuclear research
CNS	central nervous system
COX2	Cyclooxygenase-2
CSF1R	Colony-stimulating factor-1receptor
CT	Computer tomography
DC	Dendritic cell
DLD	Dihydrolipoyl dehydrogenase
DSB	Double-strand break
DNA	Deoxyribonucleic acid
ESRF	European synchrotron radiation facility
FBA	Fructose bisphosphate aldolase
FLASH	Ultra-high dose rate radiotherapy
FT-IR	Fourier-transform infrared microscopy
Gamma (γ)-H2AX	phosphorylated histone H2AX
GRID RT	Type of SFRT
Gy	Gray (unit of ionising radiation dose)
HRS	Hyper radiosensitivity
HSP-71	Heat shock protein 71
ID17	ESRF biomedical beamline
IL-8	Interleukin-8
IL-10	Interleukin-10
IMBL	Imaging and medical beamline
IR	Ionising radiation
IRR	Increased radioresistance
KeV, MeV, GeV	kiloelectron volts, megaelectron volts, gigaelectron volts (a unit of energy)
LHC	Large hadron collider
LINAC	Linear accelerator
MeJA	Methyl jasmonate
MeSA	Methyl salicylate
MDM2	mouse double minute 2 homolog
MISTRAL	Full-field transmission X-ray microscopy beamline
MRT	Microbeam radiotherapy
NAD (P)H oxidase	nicotinamide adenine dinucleotide phosphate oxidase
NK	natural killer cells
NSG	NOD SCID gamma
NSLS	National synchrotron light source
OCDL	Oxidative clustered DNA lesion
PB	Pencil beam
PSICHE	Pressure, structure and imaging by contrast at high energy beamline
Ptch1	Patched 1
RIAE	Radiation induced abscopal effect
RIBE	Radiation induced bystander effect
ROS	Reactive oxygen species
RT	Radiotherapy
SCC	Squamous cell carcinoma
SFRT	spatially fractionated radiotherapy
SYRMEP	Synchrotron radiation for medical physics beamline
TAM	Tissue-associated macrophages

TGF β	Tumour growth factor β
TGF β R1	Tumour growth factor β receptor 1
TIMP1	Tissue inhibitor matrix metalloproteinase 1
TNF- α	Tumor necrosis factor- α
TP53	Tumor protein 53
TPI	Triosephosphate isomerase
UVC	Ultraviolet C
VEGF	Vascular endothelial growth factor
WT	wild type
XRD-CT	X-ray diffraction tomography

References

1. Pełka, J. Synchrotron radiation in biology and medicine. *Acta Phys. Pol. A* **2008**, *2*, 309–329. [[CrossRef](#)]
2. Stevenson, A.W.; Crosbie, J.C.; Hall, C.J.; Hausermann, D.; Livingstone, J.; Lye, J.E. Quantitative characterization of the X-ray beam at the Australian Synchrotron Imaging and Medical Beamline (IMBL). *J. Synchrotron Radiat.* **2017**, *24*, 110–141. [[CrossRef](#)] [[PubMed](#)]
3. Pelliccioli, P.; Donzelli, M.; Davis, J.A.; Esteve, F.; Hugtenburg, R.; Guatelli, S.; Petasecca, M.; Lerch, M.L.F.; Brauer-Krisch, E.; Krisch, M. Study of the X-ray radiation interaction with a multislit collimator for the creation of microbeams in radiation therapy. *J. Synchrotron Radiat.* **2021**, *28*, 392–403. [[CrossRef](#)] [[PubMed](#)]
4. Raj, V.; Rai, A.; Sharma, S. Role of synchrotron radiation in cancer: A review on techniques and applications. *Engl. J. Anal. Pharm. Res.* **2018**, *7*, 175–180. [[CrossRef](#)]
5. Wilson, J.D.; Hammond, E.M.; Higgins, G.S.; Petersson, K. Ultra-High Dose Rate (FLASH) Radiotherapy: Silver Bullet or Fool's Gold? *Front. Oncol.* **2020**, *9*, 1563. [[CrossRef](#)]
6. Smyth, L.M.; Senthil, S.; Crosbie, J.C.; Rogers, P.A. The normal tissue effects of microbeam radiotherapy: What do we know, and what do we need to know to plan a human clinical trial? *Int. J. Radiat. Biol.* **2016**, *92*, 302–311. [[CrossRef](#)]
7. Bharti, A.; Goyal, N. Fundamental of Synchrotron Radiations. In *Synchrotron Radiation-Useful and Interesting Applications*; IntechOpen: London, UK, 2019.
8. Laissue, J.A.; Geiser, G.; Spanne, P.O.; Dilmanian, F.A.; Gebbers, J.O.; Geiser, M.; Wu, X.Y.; Makar, M.S.; Micca, P.L.; Nawrocky, M.M.; et al. Neuropathology of ablation of rat gliosarcomas and contiguous brain tissues using a microplanar beam of synchrotron-wiggler-generated X rays. *Int. J. Cancer* **1998**, *78*, 654–660. [[CrossRef](#)]
9. Sprung, C.N.; Cholewa, M.; Usami, N.; Kobayashi, K.; Crosbie, J.C. DNA damage and repair kinetics after microbeam radiation therapy emulation in living cells using monoenergetic synchrotron X-ray microbeams. *J. Synchrotron Radiat.* **2011**, *18*, 630–636. [[CrossRef](#)]
10. Hausermann, D.; Hall, C.; Maksimenko, A.; Campbell, C. The Imaging and Medical Beam Line at the Australian Synchrotron. *AIP Conf. Proc.* **2010**, *1266*, 3–9. [[CrossRef](#)]
11. Livingstone, J.; Adam, J.-F.; Crosbie, J.C.; Hall, C.J.; Lye, J.E.; McKinlay, J.; Pelliccia, D.; Pouzoulet, F.; Prezado, Y.; Stevenson, A.W. Preclinical radiotherapy at the Australian Synchrotron's Imaging and Medical Beamline: Instrumentation, dosimetry and a small-animal feasibility study. *J. Synchrotron Radiat.* **2017**, *24*, 854–865. [[CrossRef](#)]
12. Trappetti, V.; Fernandez-Palomo, C.; Smyth, L.; Klein, M.; Haberthur, D.; Butler, D.; Barnes, M.; Shintani, N.; de Veer, M.; Laissue, J.A.; et al. Synchrotron Microbeam Radiotherapy for the treatment of lung carcinoma: A pre-clinical study. *Int. J. Radiat. Oncol. Biol. Phys.* **2021**. [[CrossRef](#)]
13. Crosbie, J.C.; Fournier, P.; Bartzsch, S.; Donzelli, M.; Cornelius, I.; Stevenson, A.W.; Requardt, H.; Brauer-Krisch, E. Energy spectra considerations for synchrotron radiotherapy trials on the ID17 bio-medical beamline at the European Synchrotron Radiation Facility. *J. Synchrotron Radiat.* **2015**, *22*, 1035–1041. [[CrossRef](#)]
14. Duncan, M.; Donzelli, M.; Pelliccioli, P.; Brauer-Krisch, E.; Davis, J.A.; Lerch, M.L.F.; Rosenfeld, A.B.; Petasecca, M. First experimental measurement of the effect of cardio-synchronous brain motion on the dose distribution during microbeam radiation therapy. *Med. Phys.* **2020**, *47*, 213–222. [[CrossRef](#)] [[PubMed](#)]
15. Bourhis, J.; Montay-Gruel, P.; Goncalves Jorge, P.; Bailat, C.; Petit, B.; Ollivier, J.; Jeanneret-Sozzi, W.; Ozsahin, M.; Bochud, F.; Moeckli, R.; et al. Clinical translation of FLASH radiotherapy: Why and how? *Radiother. Oncol. J. Eur. Soc. Ther. Radiol. Oncol.* **2019**, *139*, 11–17. [[CrossRef](#)] [[PubMed](#)]
16. Montay-Gruel, P.; Bouchet, A.; Jaccard, M.; Patin, D.; Serduc, R.; Aim, W.; Petersson, K.; Petit, B.; Bailat, C.; Bourhis, J.; et al. X-rays can trigger the FLASH effect: Ultra-high dose-rate synchrotron light source prevents normal brain injury after whole brain irradiation in mice. *Radiother. Oncol. J. Eur. Soc. Ther. Radiol. Oncol.* **2018**, *129*, 582–588. [[CrossRef](#)] [[PubMed](#)]
17. de Kruijff, R.M. FLASH radiotherapy: Ultra-high dose rates to spare healthy tissue. *Int. J. Radiat. Biol.* **2020**, *96*, 419–423. [[CrossRef](#)]
18. Favaudon, V.; Caplier, L.; Monceau, V.; Pouzoulet, F.; Sayarath, M.; Fouillade, C.; Poupon, M.F.; Brito, I.; Hupe, P.; Bourhis, J.; et al. Ultrahigh dose-rate FLASH irradiation increases the differential response between normal and tumor tissue in mice. *Sci. Transl. Med.* **2014**, *6*, 245ra293. [[CrossRef](#)] [[PubMed](#)]

19. Vozenin, M.C.; De Fornel, P.; Petersson, K.; Favaudon, V.; Jaccard, M.; Germond, J.F.; Petit, B.; Burki, M.; Ferrand, G.; Patin, D.; et al. The Advantage of FLASH Radiotherapy Confirmed in Mini-pig and Cat-cancer Patients. *Clin. Cancer Res. Off. J. Am. Assoc. Cancer Res.* **2019**, *25*, 35–42. [[CrossRef](#)]
20. Eling, L.; Bouchet, A.; Nemoz, C.; Djonov, V.; Balosso, J.; Laissue, J.; Bräuer-Krisch, E.; Adam, J.F.; Serduc, R. Ultra high dose rate Synchrotron Microbeam Radiation Therapy. Preclinical evidence in view of a clinical transfer. *Radiother. Oncol.* **2019**, *139*, 56–61. [[CrossRef](#)]
21. Smyth, L.M.L.; Donoghue, J.F.; Ventura, J.A.; Livingstone, J.; Bailey, T.; Day, L.R.J.; Crosbie, J.C.; Rogers, P.A.W. Comparative toxicity of synchrotron and conventional radiation therapy based on total and partial body irradiation in a murine model. *Sci. Rep.* **2018**, *8*, 12044. [[CrossRef](#)]
22. Schultke, E.; Balosso, J.; Breslin, T.; Cavaletti, G.; Djonov, V.; Esteve, F.; Grotzer, M.; Hildebrandt, G.; Valdman, A.; Laissue, J. Microbeam radiation therapy—Grid therapy and beyond: A clinical perspective. *Br. J. Radiol.* **2017**, *90*, 20170073. [[CrossRef](#)] [[PubMed](#)]
23. Fernandez-Palomo, C.; Fazzari, J.; Trappetti, V.; Smyth, L.; Janka, H.; Laissue, J.; Djonov, V. Animal Models in Microbeam Radiation Therapy: A Scoping Review. *Cancers* **2020**, *12*, 527. [[CrossRef](#)] [[PubMed](#)]
24. Dilmanian, F.A.; Qu, Y.; Feinendegen, L.E.; Pena, L.A.; Bacarian, T.; Henn, F.A.; Kalef-Ezra, J.; Liu, S.; Zhong, Z.; McDonald, J.W. Tissue-sparing effect of x-ray microplanar beams particularly in the CNS: Is a bystander effect involved? *Exp. Hematol.* **2007**, *35*, 69–77. [[CrossRef](#)] [[PubMed](#)]
25. Potez, M.; Fernandez-Palomo, C.; Bouchet, A.; Trappetti, V.; Donzelli, M.; Krisch, M.; Laissue, J.; Volarevic, V.; Djonov, V. Synchrotron Microbeam Radiation Therapy as a New Approach for the Treatment of Radioresistant Melanoma: Potential Underlying Mechanisms. *Int. J. Radiat. Oncol. Biol. Phys.* **2019**, *105*, 1126–1136. [[CrossRef](#)] [[PubMed](#)]
26. Fernandez-Palomo, C.; Trappetti, V.; Potez, M.; Pellicoli, P.; Krisch, M.; Laissue, J.; Djonov, V. Complete Remission of Mouse Melanoma after Temporally Fractionated Microbeam Radiotherapy. *Cancers* **2020**, *12*, 2656. [[CrossRef](#)]
27. Wright, M.D. Microbeam radiosurgery: An industrial perspective. *Phys. Med.* **2015**, *31*, 601–606. [[CrossRef](#)]
28. Griffin, R.J.; Ahmed, M.M.; Amendola, B.; Belyakov, O.; Bentzen, S.M.; Butterworth, K.T.; Chang, S.; Coleman, C.N.; Djonov, V.; Formenti, S.C.; et al. Understanding High-Dose, Ultra-High Dose-Rate and, Spatially Fractionated Radiotherapy. *Int. J. Radiat. Oncol. Biol. Phys.* **2020**, *107*, 766–778. [[CrossRef](#)]
29. Crosbie, J.C.; Anderson, R.L.; Rothkamm, K.; Restall, C.M.; Cann, L.; Ruwanpura, S.; Meachem, S.; Yagi, N.; Svalbe, I.; Lewis, R.A.; et al. Tumor cell response to synchrotron microbeam radiation therapy differs markedly from cells in normal tissues. *Int. J. Radiat. Oncol. Biol. Phys.* **2010**, *77*, 886–894. [[CrossRef](#)]
30. Serduc, R.; Brauer-Krisch, E.; Bouchet, A.; Renaud, L.; Brochard, T.; Bravin, A.; Laissue, J.A.; Le Duc, G. First trial of spatial and temporal fractionations of the delivered dose using synchrotron microbeam radiation therapy. *J. Synchrotron Radiat.* **2009**, *16*, 587–590. [[CrossRef](#)]
31. Uyama, A.; Kondoh, T.; Nariyama, N.; Umetani, K.; Fukumoto, M.; Shinohara, K.; Kohmura, E. A narrow microbeam is more effective for tumor growth suppression than a wide microbeam: An in vivo study using implanted human glioma cells. *J. Synchrotron Radiat.* **2011**, *18*, 671–678. [[CrossRef](#)]
32. Montay-Gruel, P.; Petersson, K.; Jaccard, M.; Boivin, G.; Germond, J.F.; Petit, B.; Doenlen, R.; Favaudon, V.; Bochud, F.; Bailat, C.; et al. Irradiation in a flash: Unique sparing of memory in mice after whole brain irradiation with dose rates above 100Gy/s. *Radiother. Oncol. J. Eur. Soc. Ther. Radiol. Oncol.* **2017**, *124*, 365–369. [[CrossRef](#)] [[PubMed](#)]
33. Sabatasso, S.; Laissue, J.A.; Hlushchuk, R.; Graber, W.; Bravin, A.; Brauer-Krisch, E.; Corde, S.; Blattmann, H.; Gruber, G.; Djonov, V. Microbeam radiation-induced tissue damage depends on the stage of vascular maturation. *Int. J. Radiat. Oncol. Biol. Phys.* **2011**, *80*, 1522–1532. [[CrossRef](#)]
34. Bronnimann, D.; Bouchet, A.; Schneider, C.; Potez, M.; Serduc, R.; Brauer-Krisch, E.; Graber, W.; von Gunten, S.; Laissue, J.A.; Djonov, V. Synchrotron microbeam irradiation induces neutrophil infiltration, thrombocyte attachment and selective vascular damage in vivo. *Sci. Rep.* **2016**, *6*, 33601. [[CrossRef](#)] [[PubMed](#)]
35. Bouchet, A.; Lemasson, B.; Christen, T.; Potez, M.; Rome, C.; Coquery, N.; Le Clec'h, C.; Moisan, A.; Brauer-Krisch, E.; Leduc, G.; et al. Synchrotron microbeam radiation therapy induces hypoxia in intracerebral gliosarcoma but not in the normal brain. *Radiother. Oncol. J. Eur. Soc. Ther. Radiol. Oncol.* **2013**, *108*, 143–148. [[CrossRef](#)] [[PubMed](#)]
36. Friedl, A.A.; Prise, K.M.; Butterworth, K.T.; Montay-Gruel, P.; Favaudon, V. Radiobiology of the FLASH effect. *Med. Phys.* **2021**, 1–21. [[CrossRef](#)] [[PubMed](#)]
37. Kanagavelu, S.; Gupta, S.; Wu, X.; Philip, S.; Wattenberg, M.M.; Hodge, J.W.; Couto, M.D.; Chung, K.D.; Ahmed, M.M. In vivo effects of lattice radiation therapy on local and distant lung cancer: Potential role of immunomodulation. *Radiat. Res.* **2014**, *182*, 149–162. [[CrossRef](#)] [[PubMed](#)]
38. Trappetti, V.; Fazzari, J.M.; Fernandez-Palomo, C.; Scheidegger, M.; Volarevic, V.; Martin, O.A.; Djonov, V.G. Microbeam Radiotherapy—A Novel Therapeutic Approach to Overcome Radioresistance and Enhance Anti-Tumour Response in Melanoma. *Int. J. Mol. Sci.* **2021**, *22*, 7755. [[CrossRef](#)]
39. Hall, E.J. The bystander effect. *Health Phys.* **2003**, *85*, 31–35. [[CrossRef](#)]
40. Prise, K.M.; O'Sullivan, J.M. Radiation-induced bystander signalling in cancer therapy. *Nat. Rev. Cancer* **2009**, *9*, 351–360. [[CrossRef](#)]

41. Mothersill, C.; Seymour, C. Medium from irradiated human epithelial cells but not human fibroblasts reduces the clonogenic survival of unirradiated cells. *Int. J. Radiat. Biol.* **1997**, *71*, 421–427. [[CrossRef](#)]
42. Azzam, E.I.; de Toledo, S.M.; Gooding, T.; Little, J.B. Intercellular communication is involved in the bystander regulation of gene expression in human cells exposed to very low fluences of alpha particles. *Radiat. Res.* **1998**, *150*, 497–504. [[CrossRef](#)] [[PubMed](#)]
43. Nagasawa, H.; Little, J.B. Induction of sister chromatid exchanges by extremely low doses of alpha-particles. *Cancer Res.* **1992**, *52*, 6394–6396. [[PubMed](#)]
44. Mothersill, C.; Seymour, C. Radiation-induced non-targeted effects: Some open questions. *Radiat. Prot. Dosim.* **2015**, *166*, 125–130. [[CrossRef](#)]
45. Kadhim, M.; Salomaa, S.; Wright, E.; Hildebrandt, G.; Belyakov, O.V.; Prise, K.M.; Little, M.P. Non-targeted effects of ionising radiation—Implications for low dose risk. *Mutat. Res.* **2013**, *752*, 84–98. [[CrossRef](#)]
46. Ahmad, S.B.; McNeill, F.E.; Byun, S.H.; Prestwich, W.V.; Mothersill, C.; Seymour, C.; Armstrong, A.; Fernandez, C. Ultra-Violet Light Emission from HPV-G Cells Irradiated with Low Let Radiation From ⁹⁰Y; Consequences for Radiation Induced Bystander Effects. *Dose Response* **2013**, *11*, 498–516. [[CrossRef](#)] [[PubMed](#)]
47. Le, M.; McNeill, F.E.; Seymour, C.; Rainbow, A.J.; Mothersill, C.E. An observed effect of ultraviolet radiation emitted from beta-irradiated HaCaT cells upon non-beta-irradiated bystander cells. *Radiat. Res.* **2015**, *183*, 279–290. [[CrossRef](#)]
48. Sprung, C.N.; Ivashkevich, A.; Forrester, H.B.; Redon, C.E.; Georgakilas, A.; Martin, O.A. Oxidative DNA damage caused by inflammation may link to stress-induced non-targeted effects. *Cancer Lett.* **2015**, *356*, 72–81. [[CrossRef](#)]
49. Bonner, W.M.; Redon, C.E.; Dickey, J.S.; Nakamura, A.J.; Sedelnikova, O.A.; Solier, S.; Pommier, Y. gammaH2AX and cancer. *Nat. Rev. Cancer* **2008**, *8*, 957–967. [[CrossRef](#)]
50. Sokolov, M.V.; Smilenov, L.B.; Hall, E.J.; Panyutin, I.G.; Bonner, W.M.; Sedelnikova, O.A. Ionizing radiation induces DNA double-strand breaks in bystander primary human fibroblasts. *Oncogene* **2005**, *24*, 7257–7265. [[CrossRef](#)]
51. Sedelnikova, O.A.; Nakamura, A.; Kovalchuk, O.; Koturbash, I.; Mitchell, S.A.; Marino, S.A.; Brenner, D.J.; Bonner, W.M. DNA double-strand breaks form in bystander cells after microbeam irradiation of three-dimensional human tissue models. *Cancer Res.* **2007**, *67*, 4295–4302. [[CrossRef](#)]
52. Dickey, J.S.; Baird, B.J.; Redon, C.E.; Sokolov, M.V.; Sedelnikova, O.A.; Bonner, W.M. Intercellular communication of cellular stress monitored by gamma-H2AX induction. *Carcinogenesis* **2009**, *30*, 1686–1695. [[CrossRef](#)] [[PubMed](#)]
53. Hei, T.K.; Zhou, H.; Ivanov, V.N.; Hong, M.; Lieberman, H.B.; Brenner, D.J.; Amundson, S.A.; Geard, C.R. Mechanism of radiation-induced bystander effects: A unifying model. *J. Pharm. Pharmacol.* **2008**, *60*, 943–950. [[CrossRef](#)] [[PubMed](#)]
54. Ivanov, V.N.; Zhou, H.; Ghandhi, S.A.; Karasic, T.B.; Yaghoubian, B.; Amundson, S.A.; Hei, T.K. Radiation-induced bystander signaling pathways in human fibroblasts: A role for interleukin-33 in the signal transmission. *Cell Signal.* **2010**, *22*, 1076–1087. [[CrossRef](#)] [[PubMed](#)]
55. Dickey, J.S.; Baird, B.J.; Redon, C.E.; Avdoshina, V.; Palchik, G.; Wu, J.; Kondratyev, A.; Bonner, W.M.; Martin, O.A. Susceptibility to bystander DNA damage is influenced by replication and transcriptional activity. *Nucleic Acids Res.* **2012**, *40*, 10274–10286. [[CrossRef](#)]
56. Narayanan, P.K.; LaRue, K.E.; Goodwin, E.H.; Lehnert, B.E. Alpha particles induce the production of interleukin-8 by human cells. *Radiat. Res.* **1999**, *152*, 57–63. [[CrossRef](#)] [[PubMed](#)]
57. Azzam, E.I.; de Toledo, S.M.; Little, J.B. Oxidative metabolism, gap junctions and the ionizing radiation-induced bystander effect. *Oncogene* **2003**, *22*, 7050–7057. [[CrossRef](#)] [[PubMed](#)]
58. Azzam, E.I.; de Toledo, S.M.; Little, J.B. Direct evidence for the participation of gap junction-mediated intercellular communication in the transmission of damage signals from alpha -particle irradiated to nonirradiated cells. *Proc. Natl. Acad. Sci. USA* **2001**, *98*, 473–478. [[CrossRef](#)]
59. Azzam, E.I.; de Toledo, S.M.; Little, J.B. Stress signaling from irradiated to non-irradiated cells. *Curr Cancer Drug Targets* **2004**, *4*, 53–64. [[CrossRef](#)]
60. Iyer, R.; Lehnert, B.E.; Svensson, R. Factors underlying the cell growth-related bystander responses to alpha particles. *Cancer Res.* **2000**, *60*, 1290–1298.
61. Shao, C.; Furusawa, Y.; Aoki, M.; Matsumoto, H.; Ando, K. Nitric oxide-mediated bystander effect induced by heavy-ions in human salivary gland tumour cells. *Int. J. Radiat. Biol.* **2002**, *78*, 837–844. [[CrossRef](#)]
62. Shao, C.; Stewart, V.; Folkard, M.; Michael, B.D.; Prise, K.M. Nitric oxide-mediated signaling in the bystander response of individually targeted glioma cells. *Cancer Res.* **2003**, *63*, 8437–8442.
63. Matsumoto, H.; Hayashi, S.; Hatashita, M.; Ohnishi, K.; Shioura, H.; Ohtsubo, T.; Kitai, R.; Ohnishi, T.; Kano, E. Induction of radioresistance by a nitric oxide-mediated bystander effect. *Radiat. Res.* **2001**, *155*, 387–396. [[CrossRef](#)]
64. Zhou, H.; Ivanov, V.N.; Gillespie, J.; Geard, C.R.; Amundson, S.A.; Brenner, D.J.; Yu, Z.; Lieberman, H.B.; Hei, T.K. Mechanism of radiation-induced bystander effect: Role of the cyclooxygenase-2 signaling pathway. *Proc. Natl. Acad. Sci. USA* **2005**, *102*, 14641–14646. [[CrossRef](#)]
65. Poon, R.C.; Agnihotri, N.; Seymour, C.; Mothersill, C. Bystander effects of ionizing radiation can be modulated by signaling amines. *Env. Res.* **2007**, *105*, 200–211. [[CrossRef](#)] [[PubMed](#)]
66. Fazzari, J.; Mersov, A.; Smith, R.; Seymour, C.; Mothersill, C. Effect of 5-hydroxytryptamine (serotonin) receptor inhibitors on the radiation-induced bystander effect. *Int. J. Radiat. Biol.* **2012**, *88*, 786–790. [[CrossRef](#)] [[PubMed](#)]

67. Lyng, F.M.; Desplanques, M.; Jella, K.K.; Garcia, A.; McClean, B. The importance of serum serotonin levels in the measurement of radiation-induced bystander cell death in HaCaT cells. *Int. J. Radiat. Biol.* **2012**, *88*, 770–772. [[CrossRef](#)]
68. Mothersill, C.; Saroya, R.; Smith, R.W.; Singh, H.; Seymour, C.B. Serum serotonin levels determine the magnitude and type of bystander effects in medium transfer experiments. *Radiat. Res.* **2010**, *174*, 119–123. [[CrossRef](#)]
69. Saroya, R.; Smith, R.; Seymour, C.; Mothersill, C. Injection of reserpine into zebrafish, prevents fish to fish communication of radiation-induced bystander signals: Confirmation in vivo of a role for serotonin in the mechanism. *Dose Response* **2009**, *8*, 317–330. [[CrossRef](#)]
70. Al-Mayah, A.H.; Irons, S.L.; Pink, R.C.; Carter, D.R.; Kadhim, M.A. Possible role of exosomes containing RNA in mediating nontargeted effect of ionizing radiation. *Radiat. Res.* **2012**, *177*, 539–545. [[CrossRef](#)]
71. Jella, K.K.; Rani, S.; O'Driscoll, L.; McClean, B.; Byrne, H.J.; Lyng, F.M. Exosomes are involved in mediating radiation induced bystander signaling in human keratinocyte cells. *Radiat. Res.* **2014**, *181*, 138–145. [[CrossRef](#)]
72. Xu, W.; Wang, T.; Xu, S.; Xu, S.; Wu, L.; Wu, Y.; Bian, P. Radiation-induced epigenetic bystander effects demonstrated in *Arabidopsis thaliana*. *Radiat. Res.* **2015**, *183*, 511–524. [[CrossRef](#)] [[PubMed](#)]
73. Azzam, E.I.; de Toledo, S.M.; Raaphorst, G.P.; Mitchel, R.E. Low-dose ionizing radiation decreases the frequency of neoplastic transformation to a level below the spontaneous rate in C3H 10T1/2 cells. *Radiat. Res.* **1996**, *146*, 369–373. [[CrossRef](#)]
74. Mothersill, C.; Seymour, C. Radiation-induced bystander effects: Evidence for an adaptive response to low dose exposures? *Dose Response* **2006**, *4*, 283–290. [[CrossRef](#)] [[PubMed](#)]
75. Matsumoto, H.; Takahashi, A.; Ohnishi, T. Radiation-induced adaptive responses and bystander effects. *Biol. Sci. Space* **2004**, *18*, 247–254. [[CrossRef](#)] [[PubMed](#)]
76. Mole, R.H. Whole body irradiation; radiobiology or medicine? *Br. J. Radiol.* **1953**, *26*, 234–241. [[CrossRef](#)] [[PubMed](#)]
77. Koturbash, I.; Rugo, R.E.; Hendricks, C.A.; Loree, J.; Thibault, B.; Kutanzi, K.; Pogribny, I.; Yanch, J.C.; Engelward, B.P.; Kovalchuk, O. Irradiation induces DNA damage and modulates epigenetic effectors in distant bystander tissue in vivo. *Oncogene* **2006**, *25*, 4267–4275. [[CrossRef](#)]
78. Koturbash, I.; Loree, J.; Kutanzi, K.; Koganow, C.; Pogribny, I.; Kovalchuk, O. In vivo bystander effect: Cranial X-irradiation leads to elevated DNA damage, altered cellular proliferation and apoptosis, and increased p53 levels in shielded spleen. *Int. J. Radiat. Oncol. Biol. Phys.* **2008**, *70*, 554–562. [[CrossRef](#)]
79. Mancuso, M.; Pasquali, E.; Leonardi, S.; Tanori, M.; Rebessi, S.; Di Majo, V.; Pazzaglia, S.; Toni, M.P.; Pimpinella, M.; Covelli, V.; et al. Oncogenic bystander radiation effects in Patched heterozygous mouse cerebellum. *Proc. Natl. Acad. Sci. USA* **2008**, *105*, 12445–12450. [[CrossRef](#)]
80. Dubrova, Y.E. Radiation-induced transgenerational instability. *Oncogene* **2003**, *22*, 7087–7093. [[CrossRef](#)]
81. Tamminga, J.; Koturbash, I.; Baker, M.; Kutanzi, K.; Kathiria, P.; Pogribny, I.P.; Sutherland, R.J.; Kovalchuk, O. Paternal cranial irradiation induces distant bystander DNA damage in the germline and leads to epigenetic alterations in the offspring. *Cell Cycle* **2008**, *7*, 1238–1245. [[CrossRef](#)]
82. Hall, E.J. Intensity-modulated radiation therapy, protons, and the risk of second cancers. *Int. J. Radiat. Oncol. Biol. Phys.* **2006**, *65*, 1–7. [[CrossRef](#)] [[PubMed](#)]
83. Demaria, S.; Ng, B.; Devitt, M.L.; Babb, J.S.; Kawashima, N.; Liebes, L.; Formenti, S.C. Ionizing radiation inhibition of distant untreated tumors (abscopal effect) is immune mediated. *Int. J. Radiat. Oncol. Biol. Phys.* **2004**, *58*, 862–870. [[CrossRef](#)] [[PubMed](#)]
84. Siva, S.; MacManus, M.P.; Martin, R.F.; Martin, O.A. Abscopal effects of radiation therapy: A clinical review for the radiobiologist. *Cancer Lett.* **2015**, *356*, 82–90. [[CrossRef](#)]
85. Abuodeh, Y.; Venkat, P.; Kim, S. Systematic review of case reports on the abscopal effect. *Curr. Probl. Cancer* **2016**, *40*, 25–37. [[CrossRef](#)] [[PubMed](#)]
86. Ko, E.C.; Benjamin, K.T.; Formenti, S.C. Generating antitumor immunity by targeted radiation therapy: Role of dose and fractionation. *Adv. Radiat. Oncol.* **2018**, *3*, 486–493. [[CrossRef](#)] [[PubMed](#)]
87. Surinov, B.P.; Isaeva, V.G.; Karpova, N.A. Post-radiation communicative induction of blood and immunity disorders. *Patol. Fiziol. Eksp. Ter.* **1998**, *3*, 7–10.
88. Mothersill, C.; Bucking, C.; Smith, R.W.; Agnihotri, N.; O'Neill, A.; Kilemade, M.; Seymour, C.B. Communication of radiation-induced stress or bystander signals between fish in vivo. *Env. Sci. Technol.* **2006**, *40*, 6859–6864. [[CrossRef](#)]
89. Mothersill, C.; Smith, R.W.; Agnihotri, N.; Seymour, C.B. Characterization of a radiation-induced stress response communicated in vivo between zebrafish. *Env. Sci. Technol.* **2007**, *41*, 3382–3387. [[CrossRef](#)]
90. Smith, R.W.; Wang, J.; Bucking, C.P.; Mothersill, C.E.; Seymour, C.B. Evidence for a protective response by the gill proteome of rainbow trout exposed to X-ray induced bystander signals. *Proteomics* **2007**, *7*, 4171–4180. [[CrossRef](#)]
91. Mothersill, C.; Smith, R.W.; Saroya, R.; Denbeigh, J.; Rowe, B.; Banevicius, L.; Timmins, R.; Moccia, R.; Seymour, C.B. Irradiation of rainbow trout at early life stages results in legacy effects in adults. *Int. J. Radiat. Biol.* **2010**, *86*, 817–828. [[CrossRef](#)]
92. Zhong, N.; Morris, G.M.; Bacarian, T.; Rosen, E.M.; Avraham Dilmanian, F. Response of rat skin to high-dose unidirectional X-ray microbeams: A histological study. *Radiat. Res.* **2003**, *160*, 133–142. [[CrossRef](#)] [[PubMed](#)]
93. Smilowitz, H.; Blattmann, H.; Bräuer-Krisch, E.; Bravin, A.; Di Michiel, M.; Gebbers, J.-O.; Hanson, A.; Lyubimova, N.; Slatkin, D.; Stepanek, J. Synergy of gene-mediated immunoprophylaxis and microbeam radiation therapy for advanced intracerebral rat 9L gliosarcomas. *J. Neuro-Oncol.* **2006**, *78*, 135–143. [[CrossRef](#)] [[PubMed](#)]

94. Kashino, G.; Kondoh, T.; Nariyama, N.; Umetani, K.; Ohigashi, T.; Shinohara, K.; Kurihara, A.; Fukumoto, M.; Tanaka, H.; Maruhashi, A.; et al. Induction of DNA double-strand breaks and cellular migration through bystander effects in cells irradiated with the slit-type microplanar beam of the spring-8 synchrotron. *Int. J. Radiat. Oncol. Biol. Phys.* **2009**, *74*, 229–236. [[CrossRef](#)]
95. Tomita, M.; Maeda, M.; Maezawa, H.; Usami, N.; Kobayashi, K. Bystander cell killing in normal human fibroblasts is induced by synchrotron X-ray microbeams. *Radiat. Res.* **2010**, *173*, 380–385. [[CrossRef](#)]
96. Maeda, M.; Tomita, M.; Usami, N.; Kobayashi, K. Bystander cell death is modified by sites of energy deposition within cells irradiated with a synchrotron X-ray microbeam. *Radiat. Res.* **2010**, *174*, 37–45. [[CrossRef](#)] [[PubMed](#)]
97. Lobachevsky, P.; Ivashkevich, A.; Forrester, H.B.; Stevenson, A.W.; Hall, C.J.; Sprung, C.N.; Martin, O.A. Assessment and Implications of Scattered Microbeam and Broadbeam Synchrotron Radiation for Bystander Effect Studies. *Radiat. Res.* **2015**, *184*, 650–659. [[CrossRef](#)] [[PubMed](#)]
98. Lobachevsky, P.; Forrester, H.B.; Ivashkevich, A.; Mason, J.; Stevenson, A.W.; Hall, C.J.; Sprung, C.N.; Djonov, V.G.; Martin, O.A. Synchrotron X-ray Radiation-Induced Bystander Effect: An Impact of the Scattered Radiation, Distance From the Irradiated Site and p53 Cell Status. *Front. Oncol.* **2021**, *11*, 685598. [[CrossRef](#)]
99. Ventura, J.A.; Donoghue, J.F.; Nowell, C.J.; Cann, L.M.; Day, L.R.J.; Smyth, L.M.L.; Forrester, H.B.; Rogers, P.A.W.; Crosbie, J.C. The gammaH2AX DSB marker may not be a suitable biodosimeter to measure the biological MRT valley dose. *Int. J. Radiat. Biol.* **2021**, *97*, 642–656. [[CrossRef](#)]
100. Hollstein, M.; Sidransky, D.; Vogelstein, B.; Harris, C.C. p53 mutations in human cancers. *Science* **1991**, *253*, 49–53. [[CrossRef](#)]
101. Speidel, D. The role of DNA damage responses in p53 biology. *Arch. Toxicol.* **2015**, *89*, 501–517. [[CrossRef](#)]
102. Williams, A.B.; Schumacher, B. p53 in the DNA-Damage-Repair Process. *Cold Spring Harb Perspect Med.* **2016**, *6*, a026070. [[CrossRef](#)] [[PubMed](#)]
103. Ventura, J.; Lobachevsky, P.N.; Palazzolo, J.S.; Forrester, H.; Haynes, N.M.; Ivashkevich, A.; Stevenson, A.W.; Hall, C.J.; Ntargaras, A.; Kotsaris, V.; et al. Localized Synchrotron Irradiation of Mouse Skin Induces Persistent Systemic Genotoxic and Immune Responses. *Cancer Res.* **2017**, *77*, 6389–6399. [[CrossRef](#)] [[PubMed](#)]
104. Redon, C.E.; Dickey, J.S.; Nakamura, A.J.; Kareva, I.G.; Naf, D.; Nowsheen, S.; Kryston, T.B.; Bonner, W.M.; Georgakilas, A.G.; Sedelnikova, O.A. Tumors induce complex DNA damage in distant proliferative tissues in vivo. *Proc. Natl. Acad. Sci. USA* **2010**, *107*, 17992–17997. [[CrossRef](#)] [[PubMed](#)]
105. Lobachevsky, P.N.; Ventura, J.; Giannakandropoulou, L.; Forrester, H.; Palazzolo, J.S.; Haynes, N.M.; Stevenson, A.W.; Hall, C.J.; Mason, J.; Pollakis, G.; et al. A Functional Immune System Is Required for the Systemic Genotoxic Effects of Localized Irradiation. *Int. J. Radiat. Oncol. Biol. Phys.* **2019**, *103*, 1184–1193. [[CrossRef](#)]
106. Deshmane, S.L.; Kremlev, S.; Amini, S.; Sawaya, B.E. Monocyte chemoattractant protein-1 (MCP-1): An overview. *J. Interf. Cytokine Res.* **2009**, *29*, 313–326. [[CrossRef](#)]
107. Conti, I.; Rollins, B.J. CCL2 (monocyte chemoattractant protein-1) and cancer. *Semin. Cancer Biol.* **2004**, *14*, 149–154. [[CrossRef](#)]
108. Fridlender, Z.G.; Kapoor, V.; Buchlis, G.; Cheng, G.; Sun, J.; Wang, L.C.; Singhal, S.; Snyder, L.A.; Albelda, S.M. Monocyte chemoattractant protein-1 blockade inhibits lung cancer tumor growth by altering macrophage phenotype and activating CD8+ cells. *Am. J. Respir. Cell Mol. Biol.* **2011**, *44*, 230–237. [[CrossRef](#)]
109. Ma, J.; Wang, Q.; Fei, T.; Han, J.D.; Chen, Y.G. MCP-1 mediates TGF-beta-induced angiogenesis by stimulating vascular smooth muscle cell migration. *Blood* **2007**, *109*, 987–994. [[CrossRef](#)]
110. Martin, O.A.; Martin, R.F. Cancer Radiotherapy: Understanding the Price of Tumor Eradication. *Front. Cell Dev. Biol.* **2020**, *8*, 261. [[CrossRef](#)]
111. Forrester, H.B.; Lobachevsky, P.N.; Stevenson, A.W.; Hall, C.J.; Martin, O.A.; Sprung, C.N. Abscopal Gene Expression in Response to Synchrotron Radiation Indicates a Role for Immunological and DNA Damage Response Genes. *Radiat. Res.* **2020**, *194*, 678–687. [[CrossRef](#)]
112. Parameswaran, N.; Patial, S. Tumor necrosis factor-alpha signaling in macrophages. *Crit. Rev. Eukaryot. Gene Expr.* **2010**, *20*, 87–103. [[CrossRef](#)] [[PubMed](#)]
113. Fernandez-Palomo, C.; Schültke, E.; Smith, R.; Bräuer-Krisch, E.; Laissue, J.; Schroll, C.; Fazzari, J.; Seymour, C.; Mothersill, C. Bystander effects in tumor-free and tumor-bearing rat brains following irradiation by synchrotron X-rays. *Int. J. Radiat. Biol.* **2013**, *89*, 445–453. [[CrossRef](#)] [[PubMed](#)]
114. Smith, R.W.; Wang, J.; Schültke, E.; Seymour, C.B.; Bräuer-Krisch, E.; Laissue, J.A.; Blattmann, H.; Mothersill, C.E. Proteomic changes in the rat brain induced by homogenous irradiation and by the bystander effect resulting from high energy synchrotron X-ray microbeams. *Int. J. Radiat. Biol.* **2013**, *89*, 118–127. [[CrossRef](#)]
115. Fernandez-Palomo, C.; Schültke, E.; Bräuer-Krisch, E.; Laissue, J.A.; Blattmann, H.; Seymour, C.; Mothersill, C. Investigation of abscopal and bystander effects in immunocompromised mice after exposure to pencilbeam and microbeam synchrotron radiation. *Health Phys.* **2016**, *111*, 149–159. [[CrossRef](#)]
116. Fernandez-Palomo, C.; Mothersill, C.; Bräuer-Krisch, E.; Laissue, J.; Seymour, C.; Schültke, E. γ -H2AX as a marker for dose deposition in the brain of wistar rats after synchrotron microbeam radiation. *PLoS ONE* **2015**, *10*, e0119924.
117. Surinov, B.P.; Isaeva, V.G.; Dukhova, N.N. Postirradiation volatile secretions of mice: Syngeneic and allogeneic immune and behavioral effects. *Bull. Exp. Biol. Med.* **2004**, *138*, 384–386. [[CrossRef](#)]
118. Zalcman, S.; Kerr, L.; Anisman, H. Immunosuppression elicited by stressors and stressor-related odors. *Brain Behav. Immun.* **1991**, *5*, 262–273. [[CrossRef](#)]

119. Yao, Y.; Danna, C.H.; Ausubel, F.M.; Kovalchuk, I. Perception of volatiles produced by UVC-irradiated plants alters the response to viral infection in naïve neighboring plants. *Plant. Signal. Behav.* **2012**, *7*, 741–745. [[CrossRef](#)]
120. Smith, R.; Wang, J.; Seymour, C.; Fernandez-Palomo, C.; Fazzari, J.; Schültke, E.; Bräuer-Krisch, E.; Laissue, J.; Schroll, C.; Mothersill, C. Homogenous and microbeam X-ray radiation induces proteomic changes in the brains of irradiated rats and in the brains of nonirradiated cage mate rats. *Dose-Response* **2018**, *16*, 1559325817750068. [[CrossRef](#)]
121. Dullin, C.; di Lillo, F.; Svetlove, A.; Albers, J.; Wagner, W.; Markus, A.; Sodini, N.; Dreossi, D.; Alves, F.; Tromba, G. Multiscale biomedical imaging at the SYRMEP beamline of Elettra—Closing the gap between preclinical research and patient applications. *Phys. Open* **2021**, *6*, 100050. [[CrossRef](#)]
122. King, A.; Guignot, N.; Zerbino, P.; Boulard, E.; Desjardins, K.; Bordessoule, M.; Leclerq, N.; Le, S.; Renaud, G.; Cerato, M. Tomography and imaging at the PSICHE beam line of the SOLEIL synchrotron. *Rev. Sci. Instrum.* **2016**, *87*, 093704. [[CrossRef](#)] [[PubMed](#)]
123. Saslow, W.M. Chapter 10—How Electric Currents Interact with Magnetic Fields. In *Electricity, Magnetism, and Light*; Saslow, W.M., Ed.; Academic Press: San Diego, CA, USA, 2002; pp. 419–459. [[CrossRef](#)]
124. Nave, R. Cyclotron Frequency. Available online: <http://hyperphysics.phy-astr.gsu.edu/hbase/magnetic/cyclot.html> (accessed on 1 February 2022).
125. L'Annunziata, M.F. 8.7. Synchrotron Radiation. In *Radioactivity*, 2nd ed.; L'Annunziata, M.F., Ed.; Elsevier: Boston, MA, USA, 2016; pp. 269–302. [[CrossRef](#)]